The Emerald Research Register for this journal is available at
www.emeraldinsight.com/researchregister

The current issue and full text archive of this journal is available at
www.emeraldinsight.com/0961-5539.htm

Received February 2003
Revised October 2003
Accepted December 2003

Convective heat transfer in plane channels with in-line mounted rectangular bars

Alvaro Valencia and Williams Calderón
Department of Mechanical Engineering, Universidad de Chile, Santiago, Chile

Keywords *Laminar flow, Heat transfer, Pressure, Channel flow*

Abstract *Flow structure and convective heat transfer in a plane channel with in-line mounted rectangular bars have been investigated for different bar sizes in the Reynolds number range corresponding to steady laminar flow to unsteady transitional flow. Numerical results are reported for the thermal entrance region with six in-line mounted bars and for the case with spatially periodic mounted bars. Data for heat transfer and pressure drop are presented for* $100 \leq Re \leq 1{,}000$ *and bar heights* $0.24 \leq d/H \leq 0.48$*. The unsteady Navier-Stokes equations and the energy equation have been solved by a finite-volume code with staggered grids combined with SIMPLEC pressure correction. Flow and heat transfer characteristics in the different rows are strongly dependent on Re and d/H. The flow structure and temperature field around the sixth row are compared qualitatively well with those calculated with periodic boundary conditions, however, the comparison of mean Nusselt number and friction factor shows differences for high Reynolds numbers.*

Nomenclature

C = Courant number, $U_{\max}\Delta\tau/\Delta X$
C_{f1} = skin friction coefficient on bottom wall, $\tau_{w1}/(1/2\rho U_0^2)$
C_{f2} = skin friction coefficient on top wall, $\tau_{w2}/(1/2\rho U_0^2)$
C_d = drag coefficient on bar, $D/(1/2\rho U_0^2\, d)$
C_l = lift coefficient on bar, $L/(1/2\rho U_0^2\, d)$
d = bar height
D = drag
f = friction factor, $(H/2P)\ \Delta p/(1/2\rho U_0^2)$
F = eddy shedding frequency
h = heat transfer coefficient
H = channel height
k = thermal conductivity
L = lift
Nu = averaged Nusselt number, hH/k
P = spatial pitch
p = pressure
PBC = periodic boundary conditions
Pr = Prandtl number, ν/α
Re = channel Reynolds number, U_0H/ν
S = Strouhal number, Fd/U_0
T_0 = reference temperature
T_W = channel wall temperature
T_B = bulk temperature
u = Cartesian velocity component in x-direction
v = Cartesian velocity component in y-direction
U_0 = channel-averaged velocity at inlet
U = non-dimensional Cartesian velocity component, u/U_0
V = non-dimensional Cartesian velocity component, v/U_0
X = non-dimensional Cartesian coordinate, x/H
Y = non-dimensional Cartesian coordinate, y/H

Greek symbols

α = thermal diffusivity
β = non-dimensional mean pressure gradient
θ = non-dimensional temperature, T/T_0

The financial support received from FONDECYT Chile under grant number 1010400 is gratefully acknowledged.

International Journal of Numerical Methods for Heat & Fluid Flow
Vol. 14 No. 7, 2004
pp. 866-878
© Emerald Group Publishing Limited
0961-5539
DOI 10.1108/09615530410546263

θ_B = non-dimensional bulk temperature
θ_w = non-dimensional channel wall temperature
ν = kinematic viscosity
τ = non-dimensional time, tU_0/H
τ_w = wall shear stress
$\Delta\tau$ = computational time step

1. Introduction

Fluid flow and heat transfer in plane channels are present in the cooling of electronic components and compact heat exchangers. An analysis shows that the channel Reynolds numbers by air cooled components are small. Often Reynolds numbers between 100 and 1,000 are of interest, which implies a nominal laminar flow, and therefore low heat transfer coefficients. One way of improving the performance of a plane channel is to introduce vortex generators, which periodically mix the flow and reduce the thermal boundary layer thickness. This includes longitudinal vortex generators in the form of winglets and delta wings, transverse vortex generators as cylinders, rectangular bars, grooved channels, ribs and fins. Fiebig (1997) reviewed the application of vortex generators in compact heat exchangers. Two-dimensional flow in a plane channel with in-line mounted rectangular bars to the approaching flow is considered in the present investigation. The bars induce unsteady transverse vortices to augment fluid mixing. These vortices have their axes transverse to the flow and are consistent with two-dimensional flow.

Suzuki *et al.* (1993) computed the flow around a square bar in a channel for bar Reynolds numbers ranging from 37.5 to 150 and bar heights ranging from 0.05 to 0.5 channel height. The computation reveals that vortex shedding shows a different pattern of motion from its counterpart formed behind a bar placed in a uniform flow. The bar height is indicated to be a major factor governing the conditions for the appearance of crisscross motion of the vortex. Breuer *et al.* (2000) presented accurate computations of the unsteady flow around a square bar of height $d/H = 1/8$ mounted in a plane channel, they calculated the critical Reynolds number based on bar height for onset of vortex shedding from the bar at $\mathrm{Re} = 40$. Saha *et al.* (2000) reported the transition to chaos in two-dimensional flow around a square bar, the flow undergoes a sequence of transitions from a steady pattern with a Reynolds number of 40 to an unsteady chaotic pattern with a Reynolds number of 600, for this reason the simulations in the present work were carried out for bar Reynolds number $\mathrm{Re_d} \leq 400$.

The aerodynamic stability of the downstream of two tandem square bars was investigated by Luo *et al.* (1999) for a Reynolds number of 2.52×10^4, they showed that for streamwise spacing between the centers of the two square bars $L/d \leq 4$ the associated turbulent flow structure between the bars is reattached and the downstream bar is subjected to a negative drag. Tatsutani *et al.* (1993) studied tandem of square bars in a channel for Reynolds numbers between 200 and 1,600 based on the downstream bar height. They observed distinct flow patterns that are dependent on a critical non-dimensional inter-bar spacing, λ_c, given by $\lambda_c = 168\ \mathrm{Re_d}^{-2/3}$. Below the critical spacing, two counter-rotating eddies formed in the gap between the square bars and vortex shedding was only observed for the downstream bar. At the critical spacing, eddy shedding was initiated for the upstream bar. A numerical investigation was conducted by Rosales *et al.* (2001) to analyze the unsteady flow field and heat transfer characteristics for a tandem pair of square bars in a laminar channel flow.

They studied drag, lift and heat transfer coefficients from the downstream heated bar due to inline and offset eddy-promoting bars. The results show that the drag coefficient and bar Nusselt number decrease as the heated bar approaches the wall.

Valencia (1998) presented numerical studies of the flow and heat transfer in a channel with a built-in tandem of two rectangular bars. Data are presented for channel Reynolds numbers ranging from 100 to 400, and longitudinal bar separation distances L/d ranging from 3 to 9. The key conclusion is that for longitudinal bar separation distances $L/d \geq 5$ the mean heat transfer enhancement is constant. Valencia (1999) studied unsteady flow and heat transfer in plane channels with periodically placed rectangular bars of height $0.5H$ on the channel axis and quantified the benefits of vortex shedding for pitches of $2.25H$, $4.25H$ and $6.25H$. Calculations were performed for Re= 100-400 ranging from steady laminar to unsteady transitional flow. A comparison of the mean Nusselt number as a function of the pumping power for the three configurations shows that for the same pumping power the heat transfer is the highest with the pitch $2.25H$.

Farhanieh *et al.* (1993) showed, with a experimental and numerical investigation for a plane channel with a grooved wall in the thermal entrance region, that local heat transfer distribution around the third and fourth groove were similar, for the investigated Reynolds number ranging from 100 to 1,760. Experimental determination of row-by-row heat transfer coefficients in offset-strip geometries for Reynolds numbers between 300 and 4,000 were made by Dejong and Jacobi (1997), they showed similar heat transfer rates after the fourth row. In a recent work, Comini *et al.* (2002) computed convective heat transfer in wavy channels in the entrance and in the fully developed region. The computed flow and temperature fields in the 15th half module was qualitatively similar to the unsteady flow and temperature fields computed in the fully developed region, however, the difference on mean Nusselt numbers was around 20 percent for Reynolds number of 1,000.

The current work is a two-dimensional numerical investigation of heat transfer in a plane channel with six in-line mounted rectangular bars in the thermal entrance region, and in the fully developed region with the bars repeated in a spatially periodic fashion. Six bar sizes have been computed and the influence of Re has been studied in detail for the case $d/H = 0.4$ in the range of $100 \leq \mathrm{Re} \leq 1,000$. The objectives of the present work are to study the fluid flow and heat transfer in a channel with periodically mounted transverse vortex generators, and we want to quantify also the differences on mean Nusselt number and friction factor calculated with periodic boundary conditions (PBC) compared with the corresponding calculated after the fifth row.

2. Mathematical model and geometry

The flow is assumed to be unsteady, two-dimensional and laminar. The conservation equations describing the flow and temperature fields are the continuity, the time-dependent Navier-Stokes equations, and the energy equation. The fluid is assumed to be Newtonian with constant properties and the dissipation terms in the energy equation are neglected. The governing non-dimensional equations are

$$\frac{\partial U}{\partial X} + \frac{\partial V}{\partial Y} = 0 \tag{1}$$

$$\frac{\partial U}{\partial \tau}+\frac{\partial}{\partial X}(U^2)+\frac{\partial}{\partial Y}(UV)=-\frac{\partial P}{\partial X}+\frac{1}{\mathrm{Re}}\left(\frac{\partial^2 U}{\partial X^2}+\frac{\partial^2 U}{\partial Y^2}\right) \tag{2}$$

$$\frac{\partial V}{\partial \tau}+\frac{\partial}{\partial X}(UV)+\frac{\partial}{\partial Y}(V^2)=-\frac{\partial P}{\partial Y}+\frac{1}{\mathrm{Re}}\left(\frac{\partial^2 V}{\partial X^2}+\frac{\partial^2 V}{\partial Y^2}\right) \tag{3}$$

$$\frac{\partial \theta}{\partial \tau}+\frac{\partial}{\partial X}(U\theta)+\frac{\partial}{\partial Y}(V\theta)=\frac{1}{\mathrm{Re}\ \mathrm{Pr}}\left(\frac{\partial^2 \theta}{\partial X^2}+\frac{\partial^2 \theta}{\partial Y^2}\right) \tag{4}$$

The velocities were non-dimensionalized with the mean velocity U_0, all lengths with the channel height H, the pressure with ρU_0^2, the temperature with the reference temperature T_0, and time with H/U_0. The channel Reynolds number Re is defined as U_0H/ν. Pr is the Prandtl number of the fluid, and in this study we take $\mathrm{Pr}=0.71$ corresponding to air.

In the analysis of the thermal entrance region, we specify fully developed velocity profile as inlet velocity in the channel. The fluid temperature at the inlet is constant. The exit boundary conditions are chosen to minimize the distortion of the unsteady vortices shed from the bars and to reduce perturbations that reflect back into the domain. We found that the wave equation was more compatible that setting the first derivatives in the axial direction equal to zero with the physics at the exit plane, i.e.

$$\frac{\partial \phi}{\partial t}+U_0\frac{\partial \phi}{\partial x}=0 \tag{5}$$

where the variable ϕ represents the independent variable U, V, or θ. Equation (5) is enforced at the exit plane for the momentum and energy equations, equations (2)-(4).

For the simulation of fully developed periodic flow, we assume periodicity of the solution over one basic unit and therefore the computational geometry is limited to this basic unit. Implicit in this treatment is the assumption that the flow is fully developed, both hydrodynamically and thermally. To enable PBC, the instantaneous non-dimensional pressure in the Navier Stokes equations (2) and (3) is decomposed into a mean part β that is assumed to vary linearly in X, and a fluctuating part P' that vary in X and Y, (Patankar *et al.*, 1977). Thus,

$$P(X,Y,\tau)=-\beta(\tau)X+P'(X,Y,\tau) \tag{6}$$

The mean pressure gradient β is adjusted every time step to satisfy the fixed mass flow condition. PBC are imposed on velocities and on the fluctuating part of the pressure.

For the periodic thermally developed domain with uniform channel walls temperature T_w as boundary condition, the temperature difference:

$$\frac{\theta(0,Y,\tau)-\theta_W}{\theta_B(0)-\theta_W}=\frac{\theta(P/H,\tau)-\theta_W}{\theta_B(P/H,\tau)-\theta_W} \tag{7}$$

can be considered to be periodic along the non-dimensional x-direction. The periodicity condition (7) enables the solution domain for the temperature problem limited to the longitudinal pitch P/H. The non-dimensional bulk temperature was calculated using the velocity and the temperature distribution with the equation:

$$\theta_B(X,\tau) = \frac{\int_0^1 |U|\theta \, dY}{\int_0^1 |U| \, dY} \tag{8}$$

Instantaneous local heat transfer will be expressed in terms of the local Nusselt number based on channel height and can be written as:

$$\mathrm{Nu}(X,\tau) = \frac{h(x,t)H}{k} = \frac{(\partial\theta/\partial Y)_{\mathrm{wall}}}{(\theta_B(X,\tau) - \theta_W)} \tag{9}$$

The instantaneous flow losses are evaluated with the friction factor defined as:

$$\beta = f = 1/2(C_{f1} + C_{f2}) + C_d \frac{d}{2P} \tag{10}$$

where C_{f1} and C_{f2} are the skin friction coefficients on the channel walls, C_d and d are the drag coefficient and the bar height, respectively.

Figure 1 schematically shows the computational domain. The plane channel has in the thermal entrance region six in-line mounted rectangular bars with a longitudinal pitch $P = 2H$, the velocity is fully developed in the inlet. The non-dimensional height of the rectangular bars d/H is varied from 0.24 to 0.48 for a constant channel Reynolds number $\mathrm{Re} = 600$. For the case with bar height of $d/H = 0.40$ the channel Reynolds number is varied from 100 to 1,000, to study the flow behavior from steady laminar to unsteady transitional flow. The case with bar height $d/H = 0.40$ in the fully developed region was simulated with PBC for different Reynolds numbers, to compare the results of heat transfer and flow losses with the obtained in the sixth row of the previous case.

3. Numerical method

The differential equations introduced above were solved numerically with an iterative finite-volume method, details of which can be found in the work of Patankar (1980).

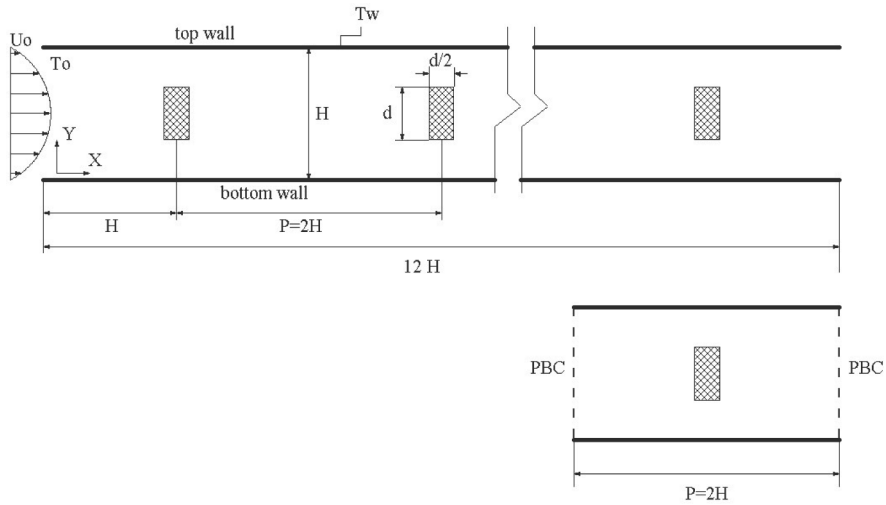

Figure 1.
Computational domain

The convection terms in the equations were approximated using a power-law scheme. The method uses staggered grids and Cartesian velocity components, handles the pressure-velocity coupling with the SIMPLEC algorithm in the form given by Van Doormaal and Raithby (1984), and solves the resulting system of equations iteratively with a tridiagonal-matrix algorithm. A first-order accurate explicit method was used for time discretization in connection with a small time step $\Delta\tau = \Delta t U_0/H = 0.001$ to capture the complex unsteady flow with a grid size of $1,200 \times 100$ control volumes for the entrance region, and with a grid size of 200×100 control volumes for the fully developed region. The time step satisfied the Courant condition, $C = 0.15$.

To check grid independence, numerical simulations of unsteady flow and heat transfer for the thermal entrance case with six in-line mounted rectangular bars of height $d/H = 0.4$ for channel Reynolds number of $\mathrm{Re} = 600$ were performed on grids of 960×80, $1,200 \times 100$, $1,440 \times 120$ and $1,680 \times 140$ control volumes. The calculation with the different grid sizes were performed with different time steps, in such a way that the Courant number of the flow was constant $C = 0.15$. Values of integral parameters as the Strouhal number of the flow, mean drag coefficients, fluctuation of lift coefficients, friction factor and mean Nusselt number on the channel walls were compared for the four different grid sizes. With the grid of $1,200 \times 100$ control volumes the differences in all the integral parameters compared with the grid of $1,680 \times 140$ control volumes were smaller than 5.0 per cent. Therefore, the grid of $1,200 \times 100$ control volumes with the time step of 0.001 will be used for the simulation of the unsteady laminar flow in the channel with in-line mounted rectangular bars.

A typical run of 8×10^4 time steps with $1,202 \times 102$ grid points takes about 72 h on a personal computer with a Pentium IV processor. To determine mean values the program should be run until a unsteady but periodic state is reached, and then the values of all fields in each 1/16 of one period are saved.

4. Results and discussion

The structure of the flow in the unsteady transitional regime will first be discussed. It can be illustrated through the use of the instantaneous velocity vectors. Figure 2 shows an instantaneous map of velocity vectors for the case $d/H = 0.4$ and $\mathrm{Re} = 600$. One can notice unsteady transverse vortices generated in the channel due to the bars, and after the third bar also unsteady vortices were found near the walls. The unsteady vortices mix core fluid with near wall fluid. The Karman vortex sheets are shed from the downstream face of the bars and travel through the channel, washing across the upstream face of the next bars. Thus, the upstream face of the bars are exposed to a periodically-induced flushing. For $\mathrm{Re} \geq 600$ and $d/H = 0.4$, two counter-rotating eddies formed in the gap between the first and second rectangular bars, and vortex shedding were only observed from the second bar.

Figure 3 shows a comparison of instantaneous velocity vectors and isotherms around the sixth bar in the thermal entrance region with instantaneous velocity vectors and isotherms calculated with PBC at the same time for the case $d/H = 0.4$ and $\mathrm{Re} = 600$. The qualitative agreement between both solutions on velocity and temperature fields is very well for this unsteady transitional flow with more than one frequency present in the flow. The Strouhal number calculated after the sixth bar in the thermal entrance case was $\mathrm{S} = 0.357$, and the corresponding calculated with PBC was $\mathrm{S} = 0.368$ for the dominant frequency.

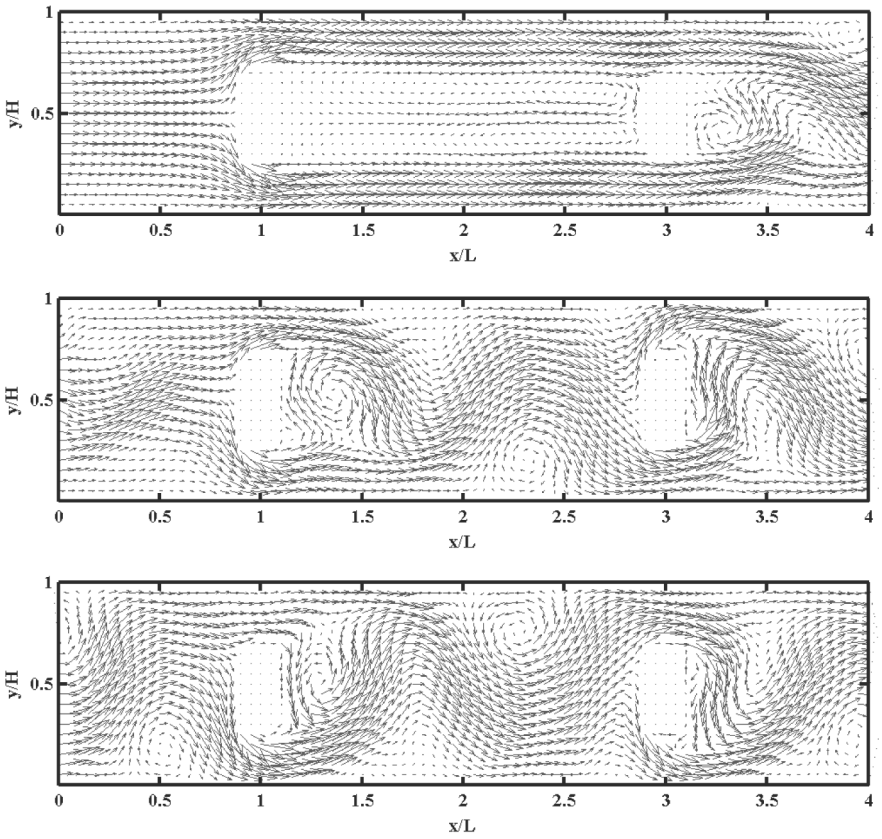

Figure 2.
Instantaneous maps of velocity vectors around the six bars for the case of $d/H = 0.4$, Re = 600 in the thermal entrance region

The critical Reynolds number for onset of unsteady vortex shedding around the bars in the case with six rectangular bars of height $d/H = 0.4$ mounted in the channel was determined with the amplitude of oscillation of lift coefficient in each bar for different channel Reynolds numbers. For Re = 100, the flow was steady with recirculation region after each bar. For Re = 125, only the lift coefficient of the sixth bar oscillates with a amplitude of 0.001 and without vortex shedding. For the critical channel Reynolds number of 150 ($Re_d = 60$), vortex shedding were observed after the second bar, the amplitude of lift coefficient varied from 0.05 to 2.6 for the first and last bar respectively, and the Strouhal number was 0.39. From Re = 175 vortex shedding were observed after each bar, the amplitude of lift coefficient varied from 0.55 to 6.0 for the first and last bar, respectively, and the Strouhal number was 0.391. With an increase of Reynolds number until Re = 200, the amplitude of lift coefficient increased from 0.76 to 7.6 for the first and last bar, respectively, and the Strouhal number was 0.396. The critical Reynolds number and the Strouhal number increase with the blockage ratio, and in this case this parameter is more than three times greater than the used one by Breuer *et al.* (2000).

Drag coefficient for the six bars in the entrance region, and drag coefficient calculated with PBC as function of channel Reynolds number are shown for $d/H = 0.4$

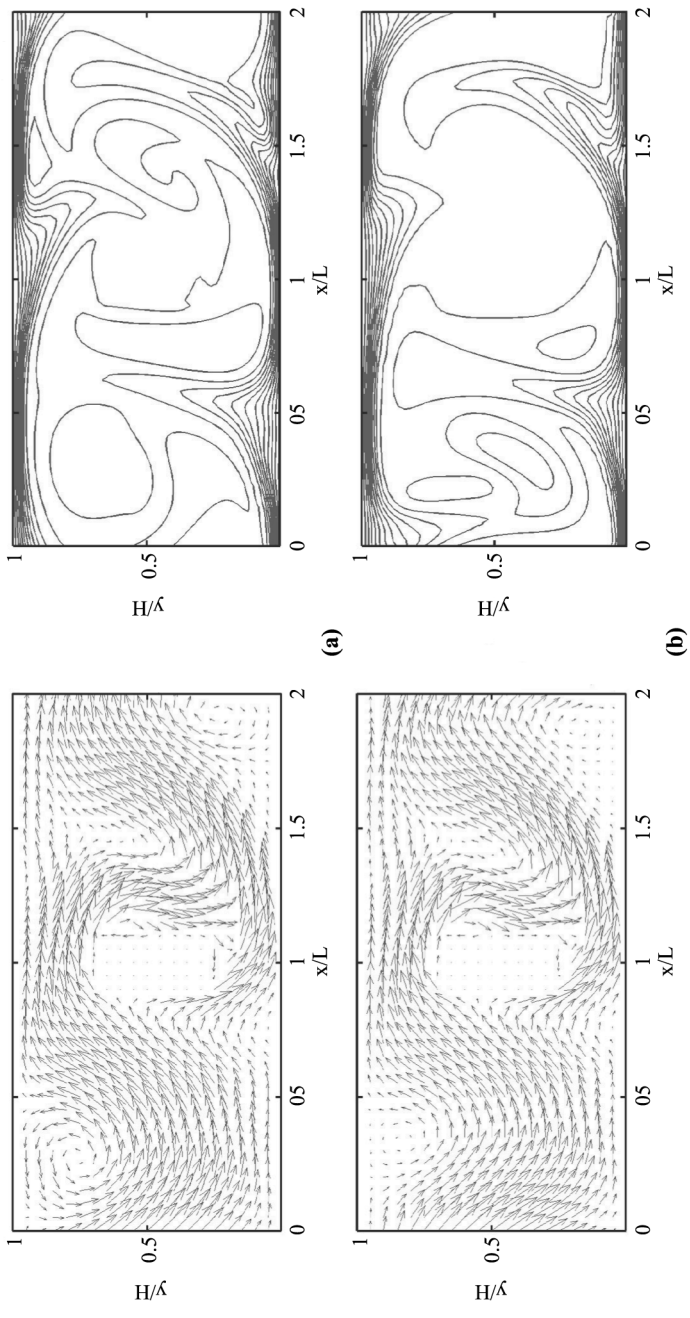

Figure 3.
Instantaneous velocity vectors and isotherms (a) around the sixth bar in the thermal entrance region and (b) calculated with PBC at the same time ($d/H = 0.4$, Re = 600)

in Figure 4. The change of flow mode between the first and second bar for $\mathrm{Re} > 500$ diminishes the drag coefficient of the second and third bars. The drag coefficient of a rectangular bar calculated with PBC is lower than the corresponding value for the sixth bar in the entrance region, and the difference increases with Re. The effects of bar height on drag coefficient for the six bars with $\mathrm{Re} = 600$ shows Figure 5. As it is expected, the drag coefficient for the first bar increases with d/H, again the change of flow mode between the first and second bar for $d/H > 0.36$ diminishes the drag coefficient of the second and third bars. In the case with $d/H = 0.48$, two counter-rotating eddies formed in the gaps between all bars, and vortex shedding were not observed in the channel, therefore, the drag coefficient for all bars was almost the same.

Figure 6 shows time averaged local Nusselt numbers on heated channel wall for three Reynolds numbers. The local Nusselt number distributions around the fifth ($8 \leq x/H \leq 10$), and sixth bar, ($10 \leq x/H \leq 12$), are practically equal, this indicates thermal fully developed conditions after four bars. For the case with vortex shedding after the first bar ($\mathrm{Re} = 500$), local Nusselt numbers for $2 \leq x/H \leq 6$ are higher than without vortex shedding after the first bar ($\mathrm{Re} > 500$). The effects of bar height on local Nusselt number distributions on heated channel wall for $\mathrm{Re} = 600$ are shown in Figure 7. As it is expected, the Nusselt number for the first row increases with d/H. Besides in the case of $d/H = 0.4$, the flow without vortex shedding after the first bar generates low local Nusselt numbers for $2 \leq x/H \leq 6$. In the case of $d/H = 0.48$ and $\mathrm{Re} = 600$ as it was mentioned earlier, vortex shedding were not observed in the channel, and therefore local Nusselt numbers were very low.

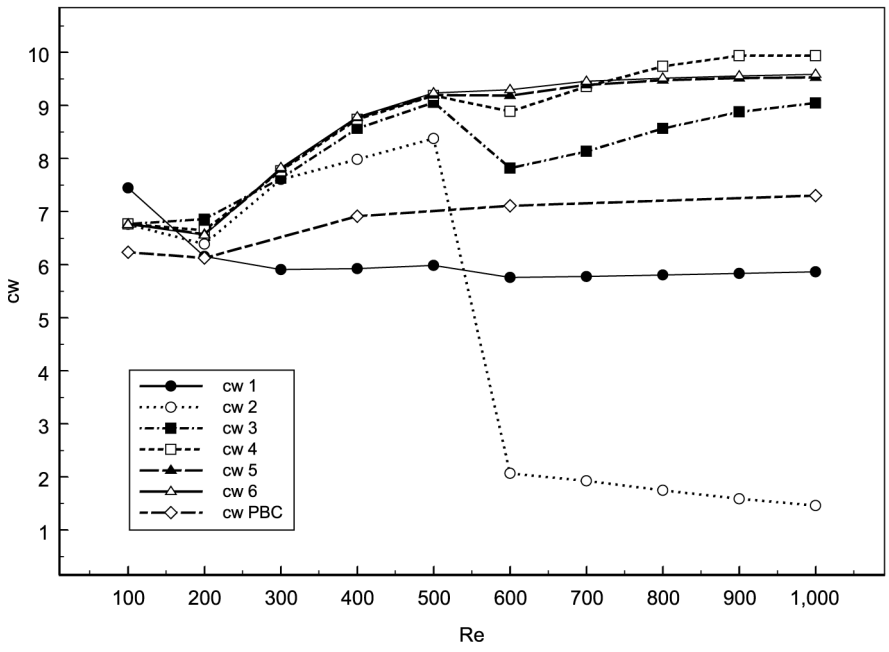

Figure 4.
Mean drag coefficients for the six bars as function of Reynolds number ($d/H = 0.4$)

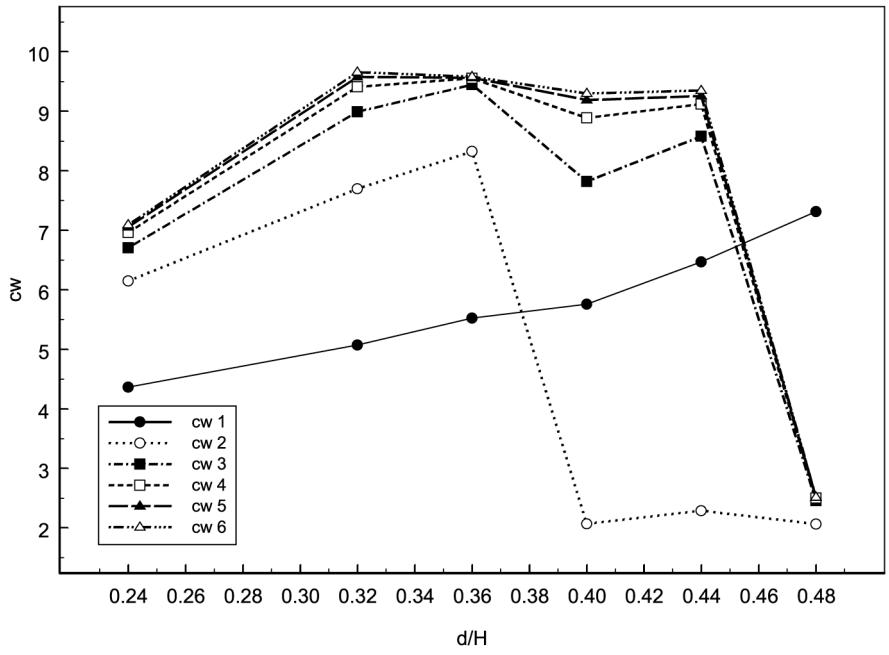

Figure 5.
Mean drag coefficients for the six bars as function of bar height (Re = 600)

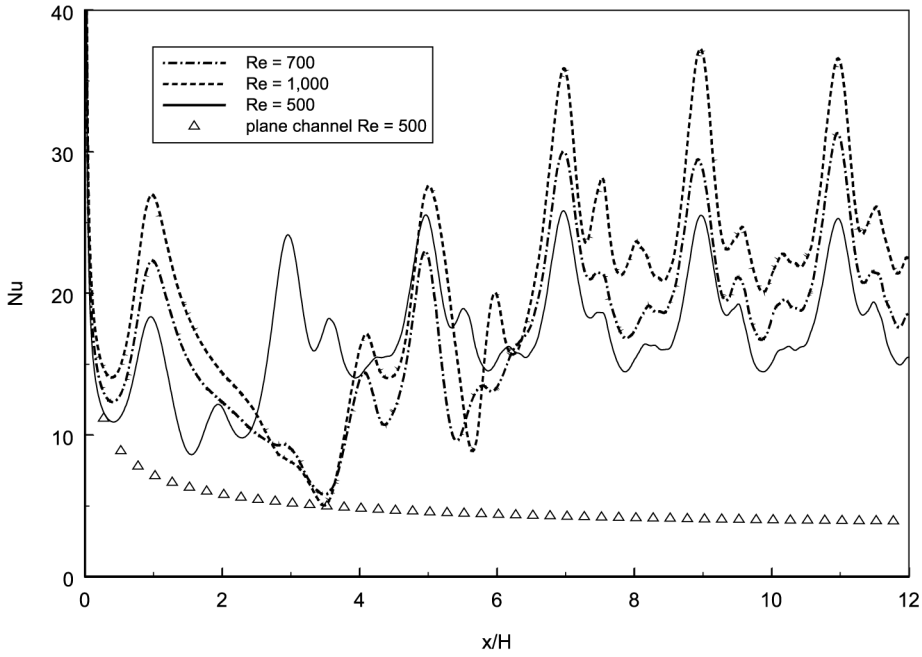

Figure 6.
Time averaged local Nusselt number on channel wall for three different Reynolds numbers ($d/H = 0.4$)

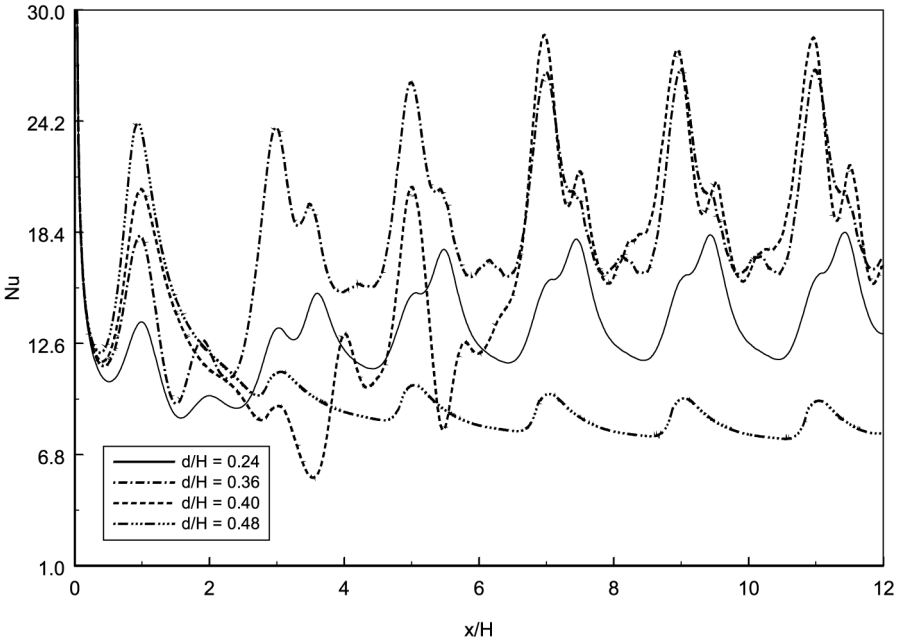

Figure 7.
Time averaged local Nusselt number on channel wall for four different bar heights (Re = 600)

Mean Nusselt number enhancement and friction factor increases as function of d/H, for the case Re = 600, are shown in Figure 8. The values obtained with $d/H = 0.48$ are very low, as in this case vortex shedding was suppressed. The heat transfer enhancement is about a factor 5.5 with friction factor increases of 57 for the case $d/H = 0.44$. Figure 9 shows mean heat transfer enhancement and friction factor increases as function of Re with $d/H = 0.4$. The influence of unsteady vortex shedding on mean heat transfer is more important than only flow deviation around the bars for high Re. The computed values with PBC are also shown, the differences between heat transfer and pressure drop obtained with thermal entrance conditions and with PBC increase with Re. For steady flow, Re = 100, both predictions are equal. For Re = 200, unsteady laminar flow, also both predictions match very well. From Re = 300 PBC predict lower heat transfer and pressure drop than calculated with the thermal entrance model after the fifth bar.

One can make a comparison of mean heat transfer between a channel with in-line periodically mounted rectangular bars and a plane channel with fully developed turbulent flow as a function of non-dimensional pumping power $f\mathrm{Re}^3$. The channel with mounted bars requires quite less pumping power than turbulent flow to achieve the same heat transport rates, because these unsteady transverse vortices yield less viscous dissipation than random chaotic turbulent fluctuations. The optimal cases are the arrangements with bar height d/H of 0.4 and 0.44.

Conclusions

Two-dimensional simulations of heat and momentum transport in a plane channel with six in-line mounted rectangular bars in the thermal entrance region, and with spatially

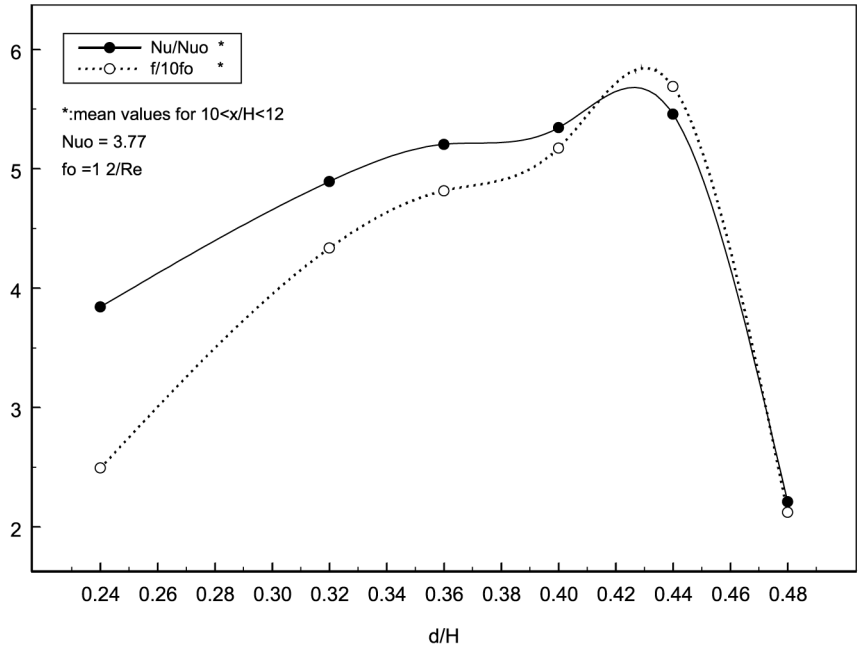

Figure 8.
Mean Nusselt number enhancement and friction factor increases as function of bar height (Re = 600)

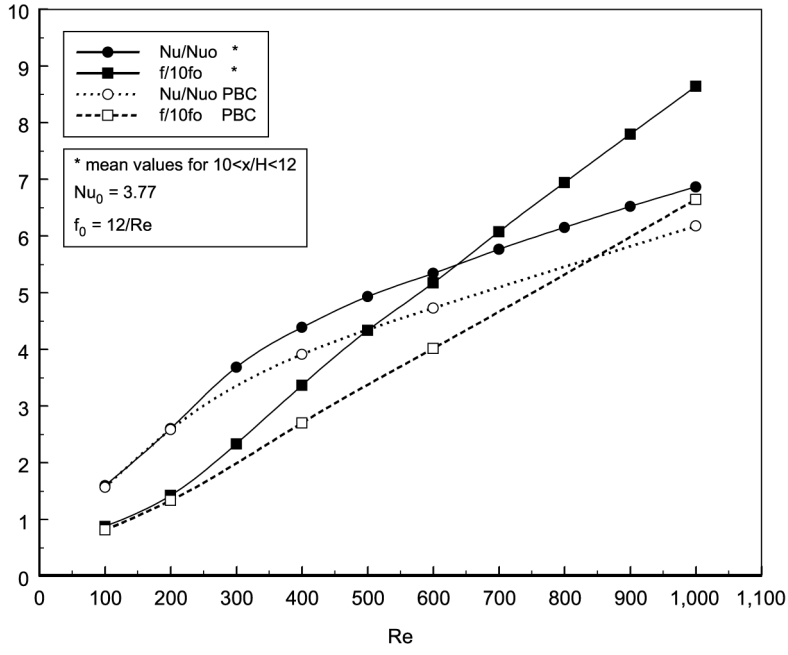

Figure 9.
Mean Nusselt number enhancement and friction factor increases as function of Reynolds number ($d/H = 0.4$)

periodic rectangular bars were performed using the finite volume technique for the channel Reynolds number range $100 \leq \mathrm{Re} \leq 1,000$, and for different bar heights. Steady flow and unsteady laminar flow as well as complex unsteady flow with transitional character depend on the Reynolds number and bar height. For high Reynolds numbers, the Nusselt number and friction factor calculated for the sixth row were higher than those obtained with PBC. The performance of the configuration was very sensitive to the choice of bar height and Reynolds number.

References

Breuer, M., Bernsdorf, J., Zeiser, T. and Durst, F. (2000), "Accurate computations of the laminar flow past a square cylinder based on two different methods: lattice-Boltzmann and finite-volume", *Int. J. Heat Fluid Flow*, Vol. 21, pp. 186-96.

Comini, G., Nonino, C. and Savino, S. (2002), "Convective heat and mass transfer in wavy finned-tube exchangers", *Int. J. Numer. Methods Heat Fluid Flow*, Vol. 12, pp. 735-55.

Dejong, N.C. and Jacobi, A.M. (1997), "An experimental study of flow and heat transfer in parallel-plate arrays: local, row-by-row and surface average behavior", *Int. J. Heat Mass Transfer*, Vol. 40, pp. 1365-78.

Farhanieh, B., Herman, Č and Sundén, B. (1993), "Numerical and experimental analysis of laminar fluid flow and forced convection heat transfer in a grooved duct", *Int. J. Heat Mass Transfer*, Vol. 36, pp. 1609-17.

Fiebig, M. (1997), "Vortices and heat transfer", *Z. für Angew. Math. Mech.*, Vol. 77, pp. 3-18.

Luo, S.C., Li, L.L. and Shah, D.A. (1999), "Aerodynamic stability of the downstream of two tandem square-section cylinders", *J. Wind Eng. Ind. Aerodyn.*, Vol. 79, pp. 79-103.

Patankar, S.V. (1980), *Numerical Heat Transfer and Fluid Flow*, Hemisphere, Washington, DC.

Patankar, S.V., Liu, C.H. and Sparrow, E.M. (1977), "Fully developed flow and heat transfer in ducts having streamwise-periodic variation of cross-sectional area", *J. Heat Transfer*, Vol. 99, pp. 180-6.

Rosales, J.L., Ortega, A. and Humphrey, J.A.C. (2001), "A numerical simulation of the convective heat transfer in confined channel flow past square cylinders: comparison of inline and offset tandem pairs", *Int. J. Heat Mass Transfer*, Vol. 44, pp. 587-603.

Saha, A.K., Muralidhar, K. and Biswas, G. (2000), "Transition and chaos in two-dimensional flow past a square cylinder", *J. Eng. Mech.*, Vol. 126, pp. 523-32.

Suzuki, H., Inoue, Y., Nishimura, T., Fukutani, K. and Suzuki, K. (1993), "Unsteady flow in a channel obstructed by a square rod (crisscross motion of vortex)", *Int. J. Heat Fluid Flow*, Vol. 14, pp. 2-9.

Tatsutani, K., Devarakonda, R. and Humphrey, J.A.C. (1993), "Unsteady flow and heat transfer for cylinder pairs in a channel", *Int. J. Heat Mass Transfer*, Vol. 36, pp. 3311-28.

Valencia, A. (1998), "Numerical study of self-sustained oscillatory flows and heat transfer in channels with a tandem of transverse vortex generators", *Heat Mass Transfer*, Vol. 33, pp. 465-70.

Valencia, A. (1999), "Heat transfer enhancement due to self-sustained oscillating transverse vortices in channels with periodically mounted rectangular bars", *Int. J. Heat Mass Transfer*, Vol. 42, pp. 2053-62.

Van Doormaal, J.P. and Raithby, G.D. (1984), "Enhancements of the SIMPLE method for predicting incompressible fluid flows", *Numer. Heat Transfer*, Vol. 7, pp. 147-63.